

# Kernel-aware Raw Burst Blind Super-Resolution

Wenyi Lian Shanglian Peng

School of Computer Science, Chengdu University of Information Technology, China

shermanlian@163.com, psl@cuit.edu.cn



Figure 1. We propose a kernel guided framework to handle the RAW burst super-resolution with multiple degradations. The proposed method outperforms existing state-of-the-art MFSR approaches DBSR [3], DeepREP [4], and EBSR [34].

## Abstract

Burst super-resolution (SR) provides a possibility of restoring rich details from low-quality images. However, since low-resolution (LR) images in practical applications have multiple complicated and unknown degradations, existing non-blind (e.g., bicubic) designed networks usually lead to a severe performance drop in recovering high-resolution (HR) images. Moreover, handling multiple misaligned noisy raw inputs is also challenging. In this paper, we address the problem of reconstructing HR images from raw burst sequences acquired from modern handheld devices. The central idea is a kernel-guided strategy which can solve the burst SR with two steps: kernel modeling and HR restoring. The former estimates burst kernels from raw inputs, while the latter predicts the super-resolved image

based on the estimated kernels. Furthermore, we introduce a kernel-aware deformable alignment module which can effectively align the raw images with consideration of the blurry priors. Extensive experiments on synthetic and real-world datasets demonstrate that the proposed method can perform favorable state-of-the-art performance in the burst SR problem.

## 1. Introduction

With the growing popularity of built-in smartphone cameras, the multi-frame super-resolution (MFSR) has drawn much attention due to its high practical potential to recover rich details from several low-quality images [3, 4, 29]. Compared with single image super-resolution (SISR), MFSR can provide complementary information from sub-

pixel shifts, avoiding aliasing artifacts and losing details [38,39]. Typically, we can explicitly model the multi-frame degradation process as:

$$\mathbf{x}_i = (\mathbf{k}_i \otimes \mathcal{T}_i \mathbf{y}) \downarrow_s + \eta_i, \quad (1)$$

where  $\mathbf{y}$  is the original HR image,  $\{\mathbf{x}_i\}_1^N$  is the observed low-resolution image bursts.  $\mathbf{k}_i$  and  $\mathcal{T}_i$  denote the blur kernel and scene motion transform, respectively.  $\otimes$  represents convolution operation and  $\downarrow_s$  is the subsequent downsampling with scale factor  $s$ .  $\eta_i$  is a white Gaussian noise that is independent to LR images.

Most existing MFSR methods assume that the blur kernels are known (e.g., bicubic) and the same for all frames [3,4,29,34]. Under this assumption, these MFSR methods can achieve dramatic performance to search for the best inverse solution for the bicubically downsampling degradation. However, they often suffer severe performance drop when applied to real-world applications of that the kernel is actually derived from cameras' intrinsic parameters that are complicated, unavailable, and inconsistent for burst frames [13,16,53]. Moreover, the blurry inputs will also make the alignment more difficult. To this end, we pay more attention to the model that tackles degradation of multiple unknown blur kernels, *i.e.* burst blind SR.

Single image blind SR has been well studied in recent works [2,16,33,52,55], which often need to sequentially estimate blur kernel (or its embedding), and then restore the SR image based on that kernel. However, the overall optimization of blind SR is usually alternating, complicated, and time-consuming [16]. Such a problem could be even more serious when facing burst blind SR, where each frame has a specific blur kernel and an irregular motion displacement. So far little work has focused on the blind property of the burst SR. The common solution is to train a deep model directly on the bicubically designed synthetic dataset, then finetunes it on another real-world dataset [3,12,29,34,37]. However, setting up a real-world dataset is always sensor-specific and is quite challenging since the images captured by smartphones and DSLR cameras (as raw LR images and HR images, respectively) have different qualities and image signal processors (ISP). And transferring the bicubically defined model to an unknown degradation model is also inefficient.

In this paper, we address these issues by proposing a kernel-aware raw burst SR method based on the multi-frame degradation model (Eq. (1)), called *KBNet*, which takes into account the inconsistencies of blur kernels between frames and can learn a practical multi-frame super-resolver using synthetic data. The *KBNet* consists of two neural networks: a kernel modeling network that estimates blur kernels of different images, and a restoring network that predicts the super-resolved image by fusing the information of all frames based on the estimated kernels. To make full

use of the degradation information from kernels, the restoring network employs adaptive kernel-aware blocks (AKAB) to extract clear features, and employs a kernel-aware deformable convolution (KAD) module to align and fuse complementary features. Our contributions are summarized as follows:

- We consider the inconsistent degradation of different frames and propose a novel kernel-aware network, named *KBNet*, for raw burst image blind super-resolution, which makes a substantial step towards developing read-world practical MFSR applications.
- We design a kernel-based restoring network that uses adaptive kernel-aware blocks and a kernel-aware deformable convolution module to restore SR images based on estimated blur kernels.
- Extensive experiments demonstrate that the proposed method can achieve SOTA performance on various synthetic datasets and real images.

## 2. Related work

### 2.1. Single Image Super-Resolution

SISR is a problem of trying to recover a high-resolution image from its degraded low-resolution version. In the past few years, numerous works [10,11,20,26,30,31,49,57] based on the neural network have achieved tremendous performance gains over the traditional SR methods. Since the pioneering work SRCNN [10], most subsequent works focus on optimizing the network architecture [8,11,28,31,57] and loss function [24,30,32,49]. These methods are difficult to apply to real-world applications due to their ill-posed nature.

### 2.2. Multi-Frame Super-Resolution

MFSR is an active area and has been well studied in the last three decades. Tsai and Huang [47] are the first that propose to tackle the MFSR problem. They propose to restore HR image in the frequency domain with known translations between frames. Since processing images in the frequency domain often causes visual artifacts, Peleg et al. [40] and Irani and Peleg [23] propose an iterative back-projection approach that sequentially estimates HR image and synthesizes LR image, and can refine SR image by minimizing reconstruction error between synthesized LR image and real LR image. Later works [1,14,17,18,41] improve this method with a maximum a posteriori (MAP) model and a regularization term. Farsui et al. [15] propose to jointly learn multi-frame demosaicking and super-resolution with that MAP framework. Takeda et al. [44,45] introduce a kernel regression technique for super-resolution and Wronski et al. [51] applies it on fusing aligned input frames of handheld cameras. Recently, several works [9,25,36] propose to

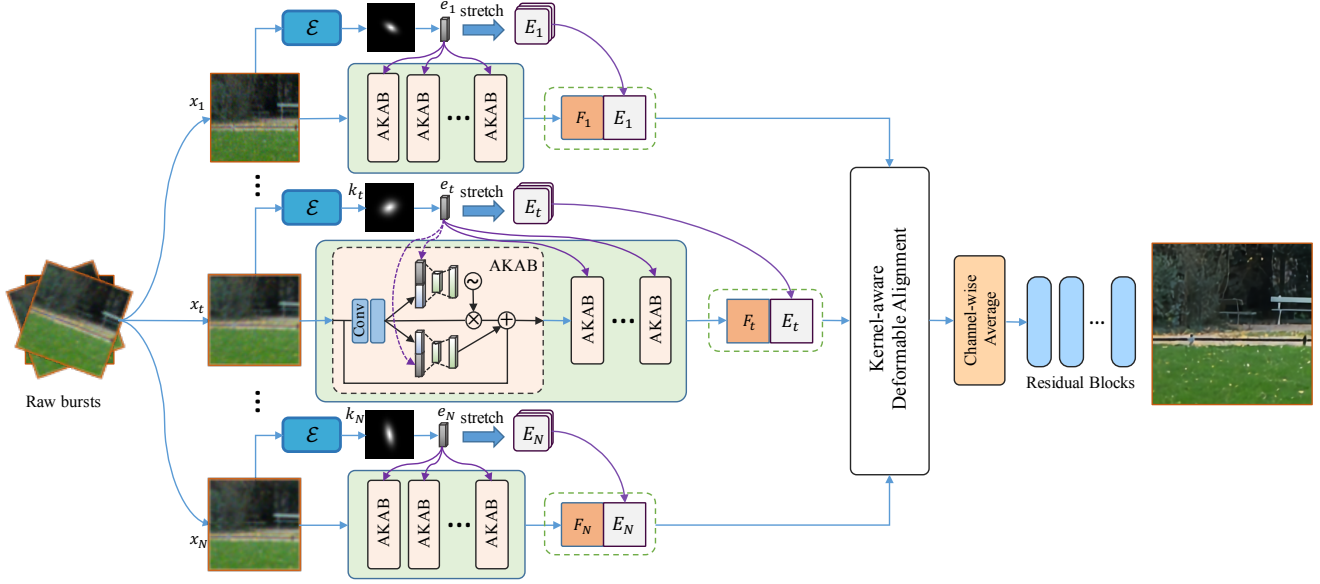


Figure 2. The overview of our method. The inputs are a set of RAW burst images  $\{x_i\}_{i=1}^N$ . We predict blur kernel for each frames through a simple CNN network, as estimator  $\mathcal{E}$ . The estimated kernels are then reduce to embeddings by PCA and fed into a groups of adaptive kernel-aware blocks to extract clean features. And we also stretch the kernel embeddings to degradation maps so as to concatenate them with clean features to align with other frames in the feature space through a kernel-aware deformable alignment module. We fuse these aligned feature using a channel-wise averaging strategy and use residual blocks to reconstruct the SR result.

incorporate deep learning to handle the MFSR problem in remote sensing applications. Bhat et al. [3] introduce a real-world dataset and propose an attention-based based fusion approach for MFSR. And they further improve the model to handle both SR and denoising by transforming the MAP framework to a deep feature space. Luo et al. [34] introduce the deformable convolution to MFSR and show its effectiveness of handling the alignment between frames. Bruno et al. [29] propose an effective hybrid algorithm building on the insight from [51]. Akshay et al. [12] propose to create a set of pseudo-burst features that makes it easier to learn distinctive information of all frames.

### 2.3. Blind Super-Resolution

Blind SR assumes that the blur kernels of degradation are unavailable. In recent years, the blind SR problem has drawn much research attention since it is close to real-world scenarios [35]. Zhang et al. [55] firstly propose to extract principal components of the Gaussian blur kernels and stretch and concatenate them with LRs to get degradation-aware SR images. Subsequently, Gu et al. [16] modify the strategy in [55] by concatenating kernel embeddings with deep features. Luo et al. [33] and Zhang et al. [54] propose to unfold the blind SR problem as a sequential two-step solution which can be alternately optimized. Hussein et al. [21] propose a closed-form correction filter to transform blurry LR images to bicubically downsampled LR im-

ages, and then the SR images can be obtained by applying existing bicubically designed CNN networks on the clear LR images. Moreover, ZSSR [2, 42] and MSSR [43] also can be applied to blind SR, where the training is conducted as test time, and it can exploit the internal information of the LR by using an image-specific degradation.

## 3. Method

This section describes the main techniques of the proposed KNet for raw burst blind SR. As shown in Fig. 2, for each frame of the raw bursts, we first estimate the blur kernel  $k_i$  by estimator  $\mathcal{E}$  and obtain its principal components embedding  $e_i$  by the principal component analysis (PCA). By taking the LR frame and the corresponding degradation kernel embedding as inputs, we can extract clean features  $F_i$  with several adaptive kernel-aware blocks (ADAB). Then we stretch kernel to degradation maps  $E_i$  with the same size as  $F_i$  so that we can concatenate the clean feature and the kernel embedding into the kernel-aware deformable (KAD) alignment module to align with other frames. After that, we fuse these aligned clean features by a channel-wise average operation and then restore the HR image like a traditional SISR model through several residual blocks.

### 3.1. Problem Formulation

Given raw burst images  $\{x_i\}_{i=1}^N$ ,  $x_i \in \mathbb{R}^{h \times w \times 1}$  captured from the same scene, our goal is to extract and fuse

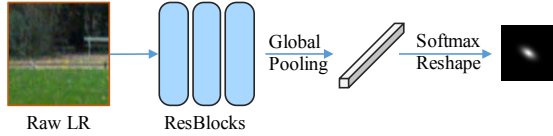


Figure 3. Network architecture of the kernel estimator.

the complementary information between them and restore a high-quality image  $y \in \mathbb{R}^{sh \times sw \times 3}$  with rich details. Here,  $s$  is the scale factor. In our scenario, each input  $x_i$  is a one-channel raw image, while the output is usually a three-channel RGB image. The degradation of burst SR is model as Eq. (1). We assume that the degradation adopts anisotropic Gaussian kernels and the noise  $\eta_i$  is independent to the LR image  $x_i$ . The burst blind SR problem can be tackled by solving the following maximum a posteriori (MAP) problem:

$$\arg \min_{k, y} \sum_{i=1}^N \|x_i - (k_i \otimes \mathcal{T}_i y)_{\downarrow s}\|_2^2 + \phi(y) + \psi(k_i), \quad (2)$$

where  $\phi(y)$  and  $\psi(k)$  are the parameterized prior regularizers. Since all of the kernels of multiple frames are unknown variables, the overall problem is extremely difficult and challenging. Inspired by recent success of single image blind SR [16, 33], we decompose this problem into two sequential steps:

$$\begin{cases} k_i = \mathcal{E}(x_i; \theta_e) \\ y = \mathcal{R}(\{x_i, k_i\}_{i=1}^N; \theta_r), \end{cases} \quad (3)$$

where  $\theta_e$  and  $\theta_r$  are the parameters of the estimator and SR network.  $\mathcal{E}(\cdot)$  denotes the kernel estimator that predicts kernels for each frame of the raw bursts.  $\mathcal{R}(\cdot)$  denotes the restorer that restores HR image based on LR frames and the estimated kernels.

### 3.2. Kernel Estimation Network

In order to find the degradation kernel that can help the SR model generate visual pleasant images. We introduce an estimator  $\mathcal{E}$  to predict blur kernels for each frame. The network architecture of the estimator is illustrated in Fig. 3. It consists of three simple steps: feature extraction, global pooling and reshape operation. Note that as a widely used kernel prior, we use the softmax function in the last so that the kernel could be sum to one. Besides, to effectively train the estimator, we provide strong supervision on the estimated kernels and ground truth kernels by minimizing the  $\mathcal{L}_1$  loss as

$$\theta_e = \arg \min_{\theta_e} \sum_{i=1}^N \|k_i - \mathcal{E}(x_i; \theta_e)\|, \quad (4)$$

By optimizing Eq. (4) with the SR model together, we are able to train the whole blind burst SR model in an end-to-end manner.

### 3.3. Adaptive Kernel-aware Block

In most blind SR methods [16, 33, 55], the estimated kernel is vectorized and reduced by PCA, and then it is stretched into a degradation map  $E_i \in \mathbb{R}^{h \times w \times m}$ , where  $m$  is the number of maintained principal components. By doing so, they can concatenate the degradation map with the LR image or features. However, such a strategy is inefficient and computationally costly [19]. Address it, we propose an adaptive kernel-aware block (AKAB) which utilizes the low-dimensional embedding and the statistical information (such as the global mean of the features) to extract clear features. Specifically, as illustrated in Fig. 2, the LR features are firstly sent to two convolution layers, and then are squeezed to one dimensional embeddings by global average pooling. After that, the feature embeddings are concatenated with kernel embeddings to perform residual affine attention which is defined as:

$$x_i^{out} = \gamma(x_i, k_i) \odot x_i + \beta(x_i, k_i) + x_i, \quad (5)$$

where  $\gamma(\cdot)$  and  $\beta(\cdot)$  denote the scaling and shifting networks, both consist of two linear layers as

$$\gamma(x_i, k_i) = g(w_2 \sigma(w_1 \mathcal{C}(e_{x_i}, e_{k_i}))), \quad (6)$$

$$\beta(x_i, k_i) = v_2 \sigma(v_1 \mathcal{C}(e_{x_i}, e_{k_i})), \quad (7)$$

where  $e_{x_i}$  and  $e_{k_i}$  represent the feature embedding and kernel embedding.  $\mathcal{C}(\cdot)$  represents the concatenation operation across the channel dimension.  $w_1, w_2$  and  $v_1, v_2$  denote linear layers for  $\gamma$  and  $\beta$ , respectively.  $\sigma$  represents a non-linear activation (e.g., ReLU), and  $g$  denotes the sigmoid function which is applied to the last layer of the scaling network  $\gamma$  as a simple gating mechanism to capture channel-wise dependencies. Moreover, the shifting network  $\beta$  is well-focused on the spatial context information of the channels and then can aggregate rich features to boost the performance.

We compose several AKABs as a powerful feature extractor so as to obtain cleaner features that implicitly embed the degradation information of kernels. Then we could align different frames in the feature level by the following kernel-aware deformable (KAD) alignment module.

### 3.4. Kernel-aware Deformable Alignment

Since deformable convolution network (DCN) has demonstrated its effectiveness of aligning features in video SR [6, 7, 46, 48], we introduce DCN into burst SR as the alignment module to effectively aggregate information from different frames. However, training DCN in our scenario is difficult since the features of the same scene may have

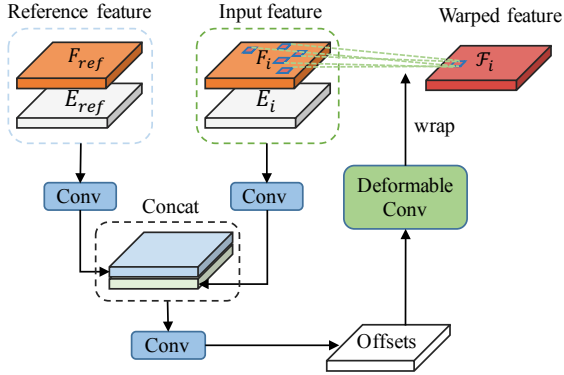


Figure 4. Network structure of the kernel-aware deformable alignment module.

different manifestations. Thus we propose to involve the degradation information into the alignment, which could guide the DCN to learn a better offset.

The overview of the KAD alignment module is shown in Fig. 4. Specifically, given a reference feature  $F_{ref}$  and another feature  $F_i$  computed from the  $i$ -th LR image and the corresponding kernel, we concatenate these features with a stretched kernel embedding  $E_{ref}$  and  $E_i$  pass through a convolution layer as kernel-aware features which can be used to obtain DCN offsets  $\Delta f_i$  as

$$\Delta f_i = \mathcal{O}(\mathcal{C}(F_{ref}, E_{ref}), \mathcal{C}(F_i, E_i)), \quad (8)$$

where  $\mathcal{O}$  is the offset predictor. Then we get the aligned feature by warping  $F_i$  with  $\Delta f_i$ :

$$\mathcal{F}_i = \mathcal{W}(F_i, \Delta f_i), \quad (9)$$

where  $\mathcal{W}$  denotes the spatial warping operation.

The KAD alignment module is jointly trained with the whole framework. We empirically choose the first frame as a reference frame and separately align each frame with it in the feature space.

### 3.5. Fusion and Reconstruction

Once the features are all aligned, we can combine information across the individual frames to generate a merged feature with rich details. Unlike previous works that use attention mechanism [3] or recursive operation [9] in the fusion, we adopt a simple yet effective channel-wise average fusion strategy as shown in Fig. 2. There are two main advantages of averaging features: firstly, the operation is fast and allows us to work with the arbitrary number of frames in both training and inference. Secondly, since the inputs are noisy, averaging all frames can reduce additional noises as a traditional denoiser. Based on the fused feature, we can reconstruct the results with advanced SR networks. The objective function of the SR reconstruction network is defined

via  $\mathcal{L}_1$  loss as:

$$\theta_r = \arg \min_{\theta_r} \|\mathbf{y} - SR(\{\mathbf{x}_i\}_{i=1}^N; \theta_r)\|. \quad (10)$$

To avoid the phenomenon of kernel mismatching [16, 55], we jointly optimize the estimator and the SR model in an end-to-end manner.

## 4. Experiments

In this section, we perform a comprehensive evaluation of the proposed method on the synthetic dataset and BurstSR dataset both introduced in [3].

### 4.1. Datasets and Implementations

#### 4.1.1 Synthetic data

Our method is trained on Zurich RAW to the RGB dataset [22] which consists of 46,839 HR images. For a synthetic dataset, we focus on the anisotropic Gaussian kernels. As the setting in [2], we fix the blur kernel size to 31, The kernel width of both axes are uniformly sampled in the range  $[0.6, 5]$ , randomly rotated by an angle uniformly distributed in  $[-\pi, \pi]$ . The RAW burst images are synthesized by randomly translating and rotating a high-quality sRGB image, and blurring and downsampling it with kernels generated from the above procedure. Then we convert the low-quality images to RAW format using an inverse camera pipeline [5]. The test sets are generated by applying anisotropic Gaussian kernels on 1204 HR images of the validation set in [22] with different kernel width ranges of  $[0.0, 1.6]$ ,  $[1.6, 3.2]$  and  $[3.2, 4.8]$ . We assign different random seed values to ensure that different blur kernels are selected for different images. PSNR and SSIM [50], as well as the learned perceptual score LPIPS [56] are used as the evaluation metrics on synthetic datasets.

#### 4.1.2 Real-world data

For real-world image evaluation, we use the BurstSR dataset which contains pairs of real-world burst images and corresponding ground truth HR images captured by a handheld smartphone camera and DCLS camera, respectively. Each burst in this dataset contains 14 raw images and is cropped to  $80 \times 80$ . To illustrate the capability of our method for real-world images, *we only take the validation dataset with 882 raw bursts for testing*. We perform super-resolution by a scale factor of 4 in all our experiments. Note that the ground truth images are not well aligned with RAW inputs, thus we adopt aligned PSNR, SSIM, and LPIPS as the evaluation metrics as introduced in [3].

#### 4.1.3 Training details

We train the proposed KNet on aforementioned synthetic datasets with 300 epochs. During training, the burst

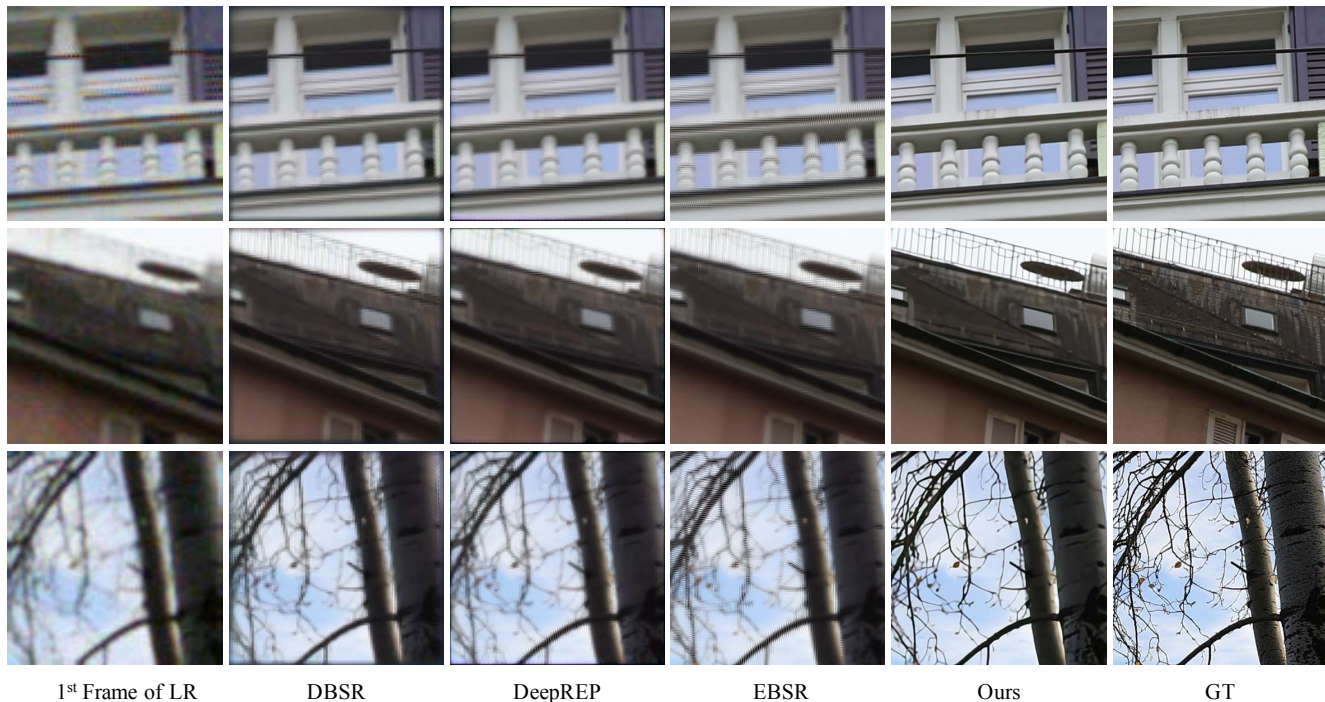


Figure 5. Visual comparison of our method with other MFSR approaches on synthetic dataset.

Method	$\sigma = [0, 1.6]$			$\sigma = [1.6, 3.2]$			$\sigma = [3.2, 4.8]$		
	PSNR $\uparrow$	SSIM $\uparrow$	LPIPS $\downarrow$	PSNR $\uparrow$	SSIM $\uparrow$	LPIPS $\downarrow$	PSNR $\uparrow$	SSIM $\uparrow$	LPIPS $\downarrow$
Single Image	32.33	0.8190	0.2316	32.06	0.8270	0.2607	31.81	0.8370	0.2994
DBSR [3]	35.40	0.9015	0.1696	33.48	0.8671	0.2612	32.03	0.8416	0.3362
EBSR [34]	35.63	0.9064	0.1673	33.69	0.8704	0.2638	32.16	0.8431	0.3399
DeepREP [4]	35.53	0.9053	0.1672	33.63	0.8702	0.2610	32.12	0.8438	0.3358
KBNet(Ours)	<b>37.15</b>	<b>0.9277</b>	<b>0.1025</b>	<b>36.62</b>	<b>0.9113</b>	<b>0.1469</b>	<b>34.28</b>	<b>0.8762</b>	<b>0.2443</b>

Table 1. Comparison of our method with existing MFSR approaches on the Synthetic  $\times 4$  test set. The kernel width  $\sigma$  is split into three ranges. We regard the single image SR method as our baseline.

size is fixed to  $N = 8$  and the batch size is 32. We use Adam [27] optimizer with  $\beta_1=0.9$ ,  $\beta_2=0.999$  and  $\epsilon=10^{-8}$ . The learning rate is initialized as 0.0002 and then decreases to half every 100 epochs. Our models are implemented by the PyTorch framework with 2 Titan Xp GPUs.

## 4.2. Comparisons with State-of-the-Art Methods

We compare KBNet with other state-of-the-art learning-based raw bursts SR methods, such as DBSR [3], EBSR [34], and DeepREP [4]. Both DBSR and DeepREP are proposed by Bhat et al. [3, 4]. The former uses a flow-based alignment network with an attention-based fusion to handle the raw burst inputs. The latter employs a deep reparametrization of the MAP to solve image restoration applications. EBSR is the winner of the NTIRE21 Burst Super-Resolution Challenge. All these methods are evaluated by using their official code and pre-trained models.

The burst size in testing is fixed to 14. We also compare a single image model which estimates a single kernel and restores the HR image conditioned on that kernel through our AKAB blocks.

### 4.2.1 Evaluation on synthetic data

Firstly, we evaluate our method on the synthetic dataset as introduced in Sec. 4.1. Quantitative results are shown in Table 1. Our method obtains the best results and outperforms other methods by a big margin. Note that each RAW frame could be blurred with an anisotropic Gaussian kernel. Thus, the single image method can not restore a pleasant SR result based on that single blurry input. While the MFSR methods can utilize the complementary information of different frames to obtain rich details. As the table illustrated, all the MFSR methods outperform single image

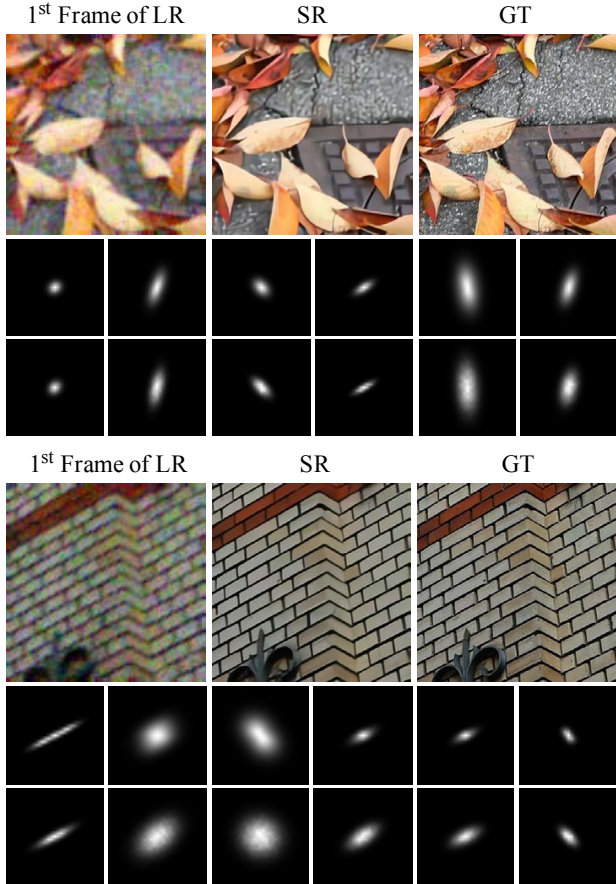


Figure 6. Two examples of estimating kernels and restoring SR image. We illustrate the first 6 kernels of the corresponding frames. For each case, top row of the kernel is the estimated kernels and second row of kernel is the ground-truth kernels.

baseline with great improvements of 3+ dB on kernels with in range  $[0, 1.6]$  in terms of PSNR. However, since most MFSR methods are designed for bicubically downsampling degradation, they are powerless to handle the blind SR problem and thus produce a relatively low performance on complex degradations. As a result, the proposed KBNet significantly outperforms the above MFSR models by a big margin over all kernel width ranges. The qualitative comparison are shown in Fig. 5. The super-resolved images produced by our KBNet are visually pleasant and clear. When the blur kernels are randomly applied to the RAW burst inputs, the MFSR methods such as DBSR, DeepREP and EBSR are tend to generate blurry results. And only our method can recover clean and sharper edges and simultaneously alleviate the blurriness. This comparison demonstrates that the involving degradation information into the multi-frame based restoration can help deblur and thus improve SR results.

Visual examples of the estimated kernel are shown in Fig. 6. As we stated in this work, frames of the same

Method	Synthetic data		
	PSNR $\uparrow$	SSIM $\uparrow$	LPIPS $\downarrow$
Baseline	35.24	0.8927	0.1751
+AKAB	36.53	0.9067	0.1422
+KAD	36.76	0.9149	0.1353

Table 2. Ablation studies on synthetic dataset. The baseline is a multi-frame SR method that adopts normal deformable convolution to align frames and reconstructs SR results by several residual blocks.

Method	BurstSR		
	PSNR $\uparrow$	SSIM $\uparrow$	LPIPS $\downarrow$
Single Image	43.33	0.9613	0.0678
DBSR [3]	44.64	0.9675	0.0789
EBSR [34]	43.32	0.9536	0.0918
DeepREP [4]	44.80	0.9688	0.0795
KBNet(Ours)	<b>45.41</b>	<b>0.9727</b>	<b>0.0379</b>

Table 3. Comparison of our method with existing MFSR approaches on the BurstSR  $\times 4$  test set.

scene are actually blurred with different complicated degradation kernels. Note that most kernels are accurately estimated by our method, which helps to restore the corresponding HR images. We also conduct ablation studies on synthetic datasets to analyze the impact of two main components in the proposed framework: adaptive kernel-aware block (AKAB) and kernel-aware deformable (KAD) alignment module. The baseline is a multi-frame SR method that adopts normal deformable convolution to align frames and reconstructs SR results by several residual blocks. The results are reported in Table 2. It is obvious that we can benefit a lot from introducing the degradation kernel. By using the AKABs, we obtain an improvement of 1.29 dB in PSNR. And the KAD further improves the result.

#### 4.2.2 Evaluation on real-world data

Then we conduct the experiment of evaluating models that trained on the synthetic dataset. The motivation of this experiment is that making paired SR datasets for real-world photography applications is really difficult. The LR RAW bursts and GT usually are captured by different cameras (for example, handheld smartphones and DSLR camera lenses). The huge differences in image quality will cause extremely low performances of image alignments across modalities. Moreover, the obtained paired images often exist severe color mismatch which may deteriorate the training. In such a situation, DBSR [3] propose to incorporate a pre-trained flow-based alignment network ( e.g., PWC-Net) and a global color mapping function to handle the spa-

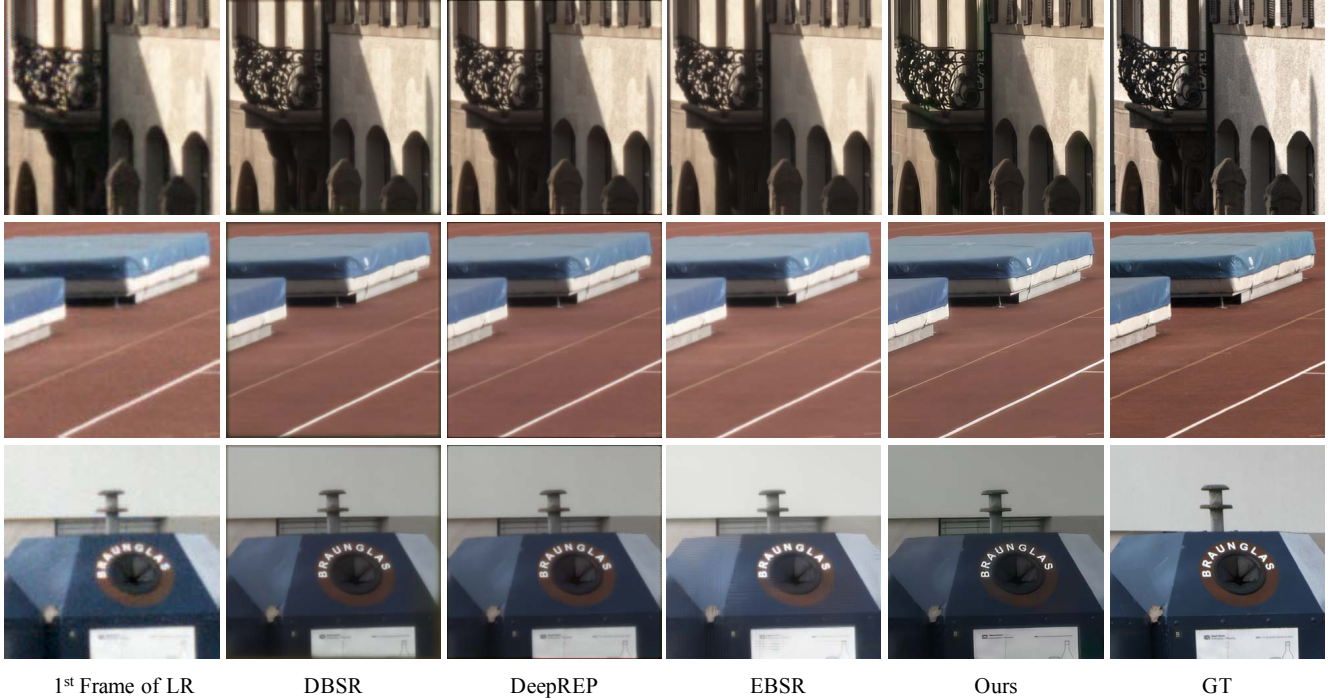


Figure 7. Visual comparison of our method with other MFSR approaches on BurstSR dataset.

tial mis-alignment and color mis-match issues. However, the pre-trained PWC-Net still can not handle complicated real-world scenes. And incorporating that model in training is time-consuming and computationally costly. Ideally, we would like to train model in a practical environment so that the trained model is able to applied to the real scenes.

As our method is proposed for various complex multi-degradation in the real world images, we directly apply the synthetically pre-trained model on the BurstSR validation set. The qualitative results are shown in Table 3. Under the blind setting, our method can perform remarkable results on real images even without any finetuning. Although DBSR and DeepREP can achieve impressive results when performing on images that have the predefined single degradation [3] (e.g., bicubic), they suffer performance drop when kernels mismatch or applied on the real-world RAW bursts. EBSR seems overfitting on the synthetic dataset and its performance is inferior to other MFSR approaches and even worse than the single image SR method. The visual results are illustrated in Fig. 7. MFSR approaches perform well on the noisy scene but are more likely to produce smoothed results and the edge is not sharp enough. Moreover, the EBSR produces unpleasant artifacts (last row in Fig. 7). Compared with these MFSR methods, the SR images generated by KNet are much sharper and cleaner. The results indicate that even if the proposed KNet is trained on synthesized image pairs, it still has the ability to generalize to

images in real applications in most cases.

## 5. Limitations

Since we add an extra network to predict the kernels for all frames, the inference time and computational costs are subsequently increased. And although our method can combine kernel estimation and burst super-resolution to achieve a good performance, it is still unsatisfied when applied to real-world applications.

## 6. Conclusion

In this paper, we present a new framework of handling multi-frame super-resolution with multiple degradations, named KNet. The proposed burst blind SR is highly related to real-world applications. Address it, we introduce a kernel-based multi-frame restoration network that includes two novel components: adaptive kernel-aware block (AKAB) and kernel-aware deformable (KAD) alignment. The blur kernels are first estimated by a simple CNN network (estimator), and then fed to the LR feature extraction module as well as feature alignment module to generate a super-resolved clear image. The proposed model network can be end-to-end trained on the synthetic dataset and evaluated on both synthetic and real-world images. Experiment results demonstrate that our method can achieve better performance on various degradations and is beneficial to real applications.



## References

- [1] Benedicte Bascle, Andrew Blake, and Andrew Zisserman. Motion deblurring and super-resolution from an image sequence. In *European conference on computer vision*, pages 571–582. Springer, 1996. [2](#)
- [2] Sefi Bell-Kligler, Assaf Shocher, and Michal Irani. Blind super-resolution kernel estimation using an internal-gan. In H. Wallach, H. Larochelle, A. Beygelzimer, F. d'Alché-Buc, E. Fox, and R. Garnett, editors, *Advances in Neural Information Processing Systems*, volume 32. Curran Associates, Inc., 2019. [2](#), [3](#), [5](#)
- [3] Goutam Bhat, Martin Danelljan, Luc Van Gool, and Radu Timofte. Deep burst super-resolution. In *Proceedings of the IEEE/CVF Conference on Computer Vision and Pattern Recognition*, pages 9209–9218, 2021. [1](#), [2](#), [3](#), [5](#), [6](#), [7](#), [8](#)
- [4] Goutam Bhat, Martin Danelljan, Fisher Yu, Luc Van Gool, and Radu Timofte. Deep reparametrization of multi-frame super-resolution and denoising. In *Proceedings of the IEEE/CVF International Conference on Computer Vision*, pages 2460–2470, 2021. [1](#), [2](#), [6](#), [7](#)
- [5] Tim Brooks, Ben Mildenhall, Tianfan Xue, Jiawen Chen, Dillon Sharlet, and Jonathan T Barron. Unprocessing images for learned raw denoising. In *Proceedings of the IEEE/CVF Conference on Computer Vision and Pattern Recognition*, pages 11036–11045, 2019. [5](#)
- [6] Kelvin CK Chan, Xintao Wang, Ke Yu, Chao Dong, and Chen Change Loy. Understanding deformable alignment in video super-resolution. *arXiv preprint arXiv:2009.07265*, 4:3, 2020. [4](#)
- [7] Kelvin CK Chan, Shangchen Zhou, Xiangyu Xu, and Chen Change Loy. Basicvsr++: Improving video super-resolution with enhanced propagation and alignment. *arXiv preprint arXiv:2104.13371*, 2021. [4](#)
- [8] Tao Dai, Jianrui Cai, Yongbing Zhang, Shu-Tao Xia, and Lei Zhang. Second-order attention network for single image super-resolution. In *Proceedings of the IEEE/CVF Conference on Computer Vision and Pattern Recognition*, pages 11065–11074, 2019. [2](#)
- [9] Michel Deudon, Alfredo Kalaitzis, Israel Goytom, Md Rifat Arefin, Zhichao Lin, Kris Sankaran, Vincent Michalski, Samira E Kahou, Julien Cornebise, and Yoshua Bengio. Highres-net: Recursive fusion for multi-frame super-resolution of satellite imagery. *arXiv preprint arXiv:2002.06460*, 2020. [2](#), [5](#)
- [10] Chao Dong, Chen Change Loy, Kaiming He, and Xiaoou Tang. Learning a deep convolutional network for image super-resolution. In *European conference on computer vision*, pages 184–199. Springer, 2014. [2](#)
- [11] Chao Dong, Chen Change Loy, Kaiming He, and Xiaoou Tang. Image super-resolution using deep convolutional networks. *IEEE transactions on pattern analysis and machine intelligence*, 38(2):295–307, 2015. [2](#)
- [12] Akshay Dudhane, Syed Waqas Zamir, Salman Khan, Fahad Khan, and Ming-Hsuan Yang. Burst image restoration and enhancement. *arXiv preprint arXiv:2110.03680*, 2021. [2](#), [3](#)
- [13] Netalee Efrat, Daniel Glasner, Alexander Apartsin, Boaz Nadler, and Anat Levin. Accurate blur models vs. image priors in single image super-resolution. In *Proceedings of the IEEE International Conference on Computer Vision*, pages 2832–2839, 2013. [2](#)
- [14] Michael Elad and Arie Feuer. Restoration of a single super-resolution image from several blurred, noisy, and undersampled measured images. *IEEE transactions on image processing*, 6(12):1646–1658, 1997. [2](#)
- [15] Sina Farsiu, Michael Elad, and Peyman Milanfar. Multi-frame demosaicing and super-resolution from undersampled color images. In *Computational Imaging II*, volume 5299, pages 222–233. International Society for Optics and Photonics, 2004. [2](#)
- [16] Jinjin Gu, Hannan Lu, Wangmeng Zuo, and Chao Dong. Blind super-resolution with iterative kernel correction. In *The IEEE Conference on Computer Vision and Pattern Recognition (CVPR)*, June 2019. [2](#), [3](#), [4](#), [5](#)
- [17] Russell C Hardie, Kenneth J Barnard, John G Bogner, Ernest E Armstrong, and Edward A Watson. High-resolution image reconstruction from a sequence of rotated and translated frames and its application to an infrared imaging system. *Optical Engineering*, 37(1):247–260, 1998. [2](#)
- [18] Muhammad Haris, Gregory Shakhnarovich, and Norimichi Ukita. Recurrent back-projection network for video super-resolution. In *Proceedings of the IEEE/CVF Conference on Computer Vision and Pattern Recognition*, pages 3897–3906, 2019. [2](#)
- [19] Zheng Hui, Jie Li, Xiumei Wang, and Xinbo Gao. Learning the non-differentiable optimization for blind super-resolution. In *Proceedings of the IEEE/CVF Conference on Computer Vision and Pattern Recognition*, pages 2093–2102, 2021. [4](#)
- [20] Zheng Hui, Xiumei Wang, and Xinbo Gao. Fast and accurate single image super-resolution via information distillation network. In *Proceedings of the IEEE conference on computer vision and pattern recognition*, pages 723–731, 2018. [2](#)
- [21] Shady Abu Hussein, Tom Tirer, and Raja Giryes. Correction filter for single image super-resolution: Robustifying off-the-shelf deep super-resolvers. In *Proceedings of the IEEE/CVF Conference on Computer Vision and Pattern Recognition*, pages 1428–1437, 2020. [3](#)
- [22] Andrey Ignatov, Luc Van Gool, and Radu Timofte. Replacing mobile camera isp with a single deep learning model. In *Proceedings of the IEEE/CVF Conference on Computer Vision and Pattern Recognition Workshops*, pages 536–537, 2020. [5](#)
- [23] Michal Irani and Shmuel Peleg. Improving resolution by image registration. *CVGIP: Graphical models and image processing*, 53(3):231–239, 1991. [2](#)
- [24] Justin Johnson, Alexandre Alahi, and Li Fei-Fei. Perceptual losses for real-time style transfer and super-resolution. In *European conference on computer vision*, pages 694–711. Springer, 2016. [2](#)
- [25] Michal Kawulok, Pawel Benecki, Krzysztof Hrynczenko, Daniel Kostrzewa, Szymon Piechaczek, Jakub Nalepa, and Bogdan Smolka. Deep learning for fast super-resolution reconstruction from multiple images. In *Real-Time Image*

- Processing and Deep Learning 2019*, volume 10996, page 109960B. International Society for Optics and Photonics, 2019. 2
- [26] Jiwon Kim, Jung Kwon Lee, and Kyoung Mu Lee. Accurate image super-resolution using very deep convolutional networks. In *Proceedings of the IEEE conference on computer vision and pattern recognition*, pages 1646–1654, 2016. 2
- [27] Diederik P Kingma and Jimmy Ba. Adam: A method for stochastic optimization. *arXiv preprint arXiv:1412.6980*, 2014. 6
- [28] Wei-Sheng Lai, Jia-Bin Huang, Narendra Ahuja, and Ming-Hsuan Yang. Deep laplacian pyramid networks for fast and accurate super-resolution. In *Proceedings of the IEEE conference on computer vision and pattern recognition*, pages 624–632, 2017. 2
- [29] Bruno Lecouat, Jean Ponce, and Julien Mairal. Lucas-kanade reloaded: End-to-end super-resolution from raw image bursts. In *Proceedings of the IEEE/CVF International Conference on Computer Vision*, pages 2370–2379, 2021. 1, 2, 3
- [30] Christian Ledig, Lucas Theis, Ferenc Huszár, Jose Caballero, Andrew Cunningham, Alejandro Acosta, Andrew Aitken, Alykhan Tejani, Johannes Totz, Zehan Wang, et al. Photo-realistic single image super-resolution using a generative adversarial network. In *Proceedings of the IEEE conference on computer vision and pattern recognition*, pages 4681–4690, 2017. 2
- [31] Bee Lim, Sanghyun Son, Heewon Kim, Seungjun Nah, and Kyoung Mu Lee. Enhanced deep residual networks for single image super-resolution. In *Proceedings of the IEEE conference on computer vision and pattern recognition workshops*, pages 136–144, 2017. 2
- [32] Andreas Lugmayr, Martin Danelljan, Luc Van Gool, and Radu Timofte. Srflo: Learning the super-resolution space with normalizing flow. In *European Conference on Computer Vision*, pages 715–732. Springer, 2020. 2
- [33] Zhengxiong Luo, Yan Huang, Shang Li, Liang Wang, and Tieniu Tan. Unfolding the alternating optimization for blind super resolution. *Advances in Neural Information Processing Systems (NeurIPS)*, 33, 2020. 2, 3, 4
- [34] Ziwei Luo, Lei Yu, Xuan Mo, Youwei Li, Lanpeng Jia, Haoqiang Fan, Jian Sun, and Shuaicheng Liu. Ebsr: Feature enhanced burst super-resolution with deformable alignment. In *Proceedings of the IEEE/CVF Conference on Computer Vision and Pattern Recognition*, pages 471–478, 2021. 1, 2, 3, 6, 7
- [35] Tomer Michaeli and Michal Irani. Nonparametric blind super-resolution. In *Proceedings of the IEEE International Conference on Computer Vision*, pages 945–952, 2013. 3
- [36] Andrea Bordone Molini, Diego Valsesia, Giulia Fracastoro, and Enrico Magli. Deepsum: Deep neural network for super-resolution of unregistered multitemporal images. *IEEE Transactions on Geoscience and Remote Sensing*, 58(5):3644–3656, 2019. 2
- [37] Rao Muhammad Umer and Christian Micheloni. Rbsr: Raw burst super-resolution through iterative convolutional neural network. In *Fourth Workshop on Machine Learning and the Physical Sciences (NeurIPS)*, December 2021. 2
- [38] Kamal Nasrollahi and Thomas B Moeslund. Super-resolution: a comprehensive survey. *Machine vision and applications*, 25(6):1423–1468, 2014. 2
- [39] Sung Cheol Park, Min Kyu Park, and Moon Gi Kang. Super-resolution image reconstruction: a technical overview. *IEEE signal processing magazine*, 20(3):21–36, 2003. 2
- [40] Shmuel Peleg, Danny Keren, and Limor Schweitzer. Improving image resolution using subpixel motion. *Pattern recognition letters*, 5(3):223–226, 1987. 2
- [41] Richard R Schultz and Robert L Stevenson. Extraction of high-resolution frames from video sequences. *IEEE transactions on image processing*, 5(6):996–1011, 1996. 2
- [42] Assaf Shocher, Nadav Cohen, and Michal Irani. “zero-shot” super-resolution using deep internal learning. In *Proceedings of the IEEE conference on computer vision and pattern recognition*, pages 3118–3126, 2018. 3
- [43] Jae Woong Soh, Sunwoo Cho, and Nam Ik Cho. Meta-transfer learning for zero-shot super-resolution. In *Proceedings of the IEEE/CVF Conference on Computer Vision and Pattern Recognition*, pages 3516–3525, 2020. 3
- [44] Hiroyuki Takeda, Sina Farsiu, and Peyman Milanfar. Robust kernel regression for restoration and reconstruction of images from sparse noisy data. In *2006 International Conference on Image Processing*, pages 1257–1260. IEEE, 2006. 2
- [45] Hiroyuki Takeda, Sina Farsiu, and Peyman Milanfar. Kernel regression for image processing and reconstruction. *IEEE Transactions on image processing*, 16(2):349–366, 2007. 2
- [46] Yapeng Tian, Yulun Zhang, Yun Fu, and Chenliang Xu. Tdan: Temporally-deformable alignment network for video super-resolution. In *Proceedings of the IEEE/CVF Conference on Computer Vision and Pattern Recognition*, pages 3360–3369, 2020. 4
- [47] R Tsai. Multiframe image restoration and registration. *Advanced Computer Visual and Image Processing*, 1:317–339, 1984. 2
- [48] Xintao Wang, Kelvin CK Chan, Ke Yu, Chao Dong, and Chen Change Loy. Edvr: Video restoration with enhanced deformable convolutional networks. In *Proceedings of the IEEE/CVF Conference on Computer Vision and Pattern Recognition Workshops*, pages 0–0, 2019. 4
- [49] Xintao Wang, Ke Yu, Shixiang Wu, Jinjin Gu, Yihao Liu, Chao Dong, Yu Qiao, and Chen Change Loy. Esrgan: Enhanced super-resolution generative adversarial networks. In *Proceedings of the European conference on computer vision (ECCV) workshops*, pages 0–0, 2018. 2
- [50] Zhou Wang, Alan C Bovik, Hamid R Sheikh, and Eero P Simoncelli. Image quality assessment: from error visibility to structural similarity. *IEEE transactions on image processing*, 13(4):600–612, 2004. 5
- [51] Bartłomiej Wronski, Ignacio Garcia-Dorado, Manfred Ernst, Damien Kelly, Michael Krainin, Chia-Kai Liang, Marc Levoy, and Peyman Milanfar. Handheld multi-frame super-resolution. *ACM Transactions on Graphics (TOG)*, 38(4):1–18, 2019. 2, 3
- [52] Yu-Syuan Xu, Shou-Yao Roy Tseng, Yu Tseng, Hsien-Kai Kuo, and Yi-Min Tsai. Unified dynamic convolutional network for super-resolution with variational degradations. In

- Proceedings of the IEEE/CVF Conference on Computer Vision and Pattern Recognition*, pages 12496–12505, 2020. [2](#)
- [53] Chih-Yuan Yang, Chao Ma, and Ming-Hsuan Yang. Single-image super-resolution: A benchmark. In *European conference on computer vision*, pages 372–386. Springer, 2014. [2](#)
- [54] Kai Zhang, Luc Van Gool, and Radu Timofte. Deep unfolding network for image super-resolution. In *Proceedings of the IEEE/CVF Conference on Computer Vision and Pattern Recognition*, pages 3217–3226, 2020. [3](#)
- [55] Kai Zhang, Wangmeng Zuo, and Lei Zhang. Learning a single convolutional super-resolution network for multiple degradations. In *Proceedings of the IEEE Conference on Computer Vision and Pattern Recognition*, pages 3262–3271, 2018. [2](#), [3](#), [4](#), [5](#)
- [56] Richard Zhang, Phillip Isola, Alexei A Efros, Eli Shechtman, and Oliver Wang. The unreasonable effectiveness of deep features as a perceptual metric. In *Proceedings of the IEEE conference on computer vision and pattern recognition*, pages 586–595, 2018. [5](#)
- [57] Yulun Zhang, Yapeng Tian, Yu Kong, Bineng Zhong, and Yun Fu. Residual dense network for image super-resolution. In *Proceedings of the IEEE conference on computer vision and pattern recognition*, pages 2472–2481, 2018. [2](#)